

OPTIMAL TUNING OF BELT CONVEYOR SOFT-STARTER VIA PSO-ROT-RING METHOD

Yuriy ROMASEVYCH¹, Viatcheslav LOVEIKIN²,
Borys BAKAY³, Ihor RUDKO⁴

In the article, a problem of optimal tuning of a soft-starter, embedded in a belt conveyor electric drive, is stated. The mathematical model used in the calculations reflects mechanical and electrical processes in the belt conveyor and its drive. In order to limit electric current in the drive and force in the belt, constraints are imposed. The criterion to minimize is energy losses in the drive. The initial problem is reduced to the unconstrained one, and a modified PSO algorithm (PSO-Rot-Ring) is applied to solve it. The solution is found in the domain of the initial value of soft-starter output voltage and the duration of voltage increase. Brief sensitivity analysis of PSO-Rot-Ring is carried out. Found optimal tuning parameters are analyzed in terms of their influence on energy and dynamical indicators of the conveyor start.

Keywords: soft-starter, belt conveyor, optimization, constraints, tuning.

1. Introduction

Belt conveyors are widely-spread machines in many areas of production, including machinery design, construction, mining, agricultural industries, etc. They are characterized by high capacity and energy efficiency. Their technical support is relatively simple. However, there are a lot of belt conveyor disadvantages. To suppress them, a belt conveyor may be equipped with a soft-starter. It controls the voltage of the electric conveyor drive during a start in such a manner, that the maximal electric current and electromagnetic torque of the drive are decreased. It, in turn, causes an increase in the belt reliability and makes energy losses of the motor during a conveyor start much smaller [1]. A soft-starter has several options, that must be tuned before its exploitation begins. There are a lot of cases, when engineers may not tune a soft-starter properly for specific conditions of operation and conveyor parameters. The solution of this problem requires scientific investigations.

In the work [2] an artificial neural network was used to develop a belt conveyor energy model. Based on that, the authors carried out optimization of the conveyor exploitation and developed a controller, which varies the belt speed with

¹ National University of Life and Environmental Sciences of Ukraine, Ukraine, e-mail, romasevichyuriy@ukr.net

² National University of Life and Environmental Sciences of Ukraine, Ukraine, e-mail: lovvs@ukr.net

³ Ukrainian National Forestry University, Ukraine, e-mail: bakay@nltu.edu.ua

⁴ Ukrainian National Forestry University, Ukraine, e-mail: ihor.rudko@nltu.edu.ua

a frequency-controlled drive. In the practice of belt conveyor utilization, bulk material may be distributed on the belt surface nonuniformly. Considering that fact researchers in the article [3] developed a multi-mass model and studied the influence of the conveyor start duration on the dynamic processes. Work [4] reveals the connection between the acceleration curve of the belt conveyor drive and the tension in the belt. Researchers recommended for application of a combined parabolic curve as the most suitable for specific exploitation conditions (long conveying distance, intermediate drive, non-uniform load distribution on the belt surface). The optimal control problem [5] addresses the belt speed varying and involves the values of electricity tariffs. To solve the problem Pontryagin maximum principle was applied. It allowed to calculate the belt speed switching moments.

There is a lot of scientific papers, where issues „soft-starter – belt conveyor drive” are studied. In the work [6] the impact of the start duration on the mechanical and energy processes of the belt conveyor was studied. For this goal, Simulink/MATLAB mathematical model was developed. Automated mechanical transmission (AMT), which is studied in the works [7, 8], may improve belt conveyor start features. In the article [7] the influence of the acceleration curves on the jerk compensation is studied. In work [8] AMT is developed to implement a segmented acceleration curve of the belt. Scientific paper [9] investigated the PI-controller tuning of the soft-starter via Ziegler-Nichols method and bio-inspired optimization methods.

Most of the mentioned studies consider only one belt conveyor exploitation factor: energy consumption, dynamical loads (for example, in the belt), capacity, etc. Another class of problems refers to the optimal soft-starter tuning (for instance, to minimize energy losses) without any connections to belt conveyor dynamics. However, it is important to stress, that improving only one class of characteristics may deteriorate others. Therefore, problems referred to belt conveyor operation should include all the essential factors (dynamic, electrical, energy, etc.).

2. Materials and Methods

The goal of the investigation is connected with the optimal tuning of a soft-starter of an asynchronous drive of a belt conveyor. In order to achieve it, a mathematical model of the electromechanical system „belt conveyor – asynchronous drive – soft-starter” should be used. A belt conveyor model (Fig. 1) was developed in the article [10].

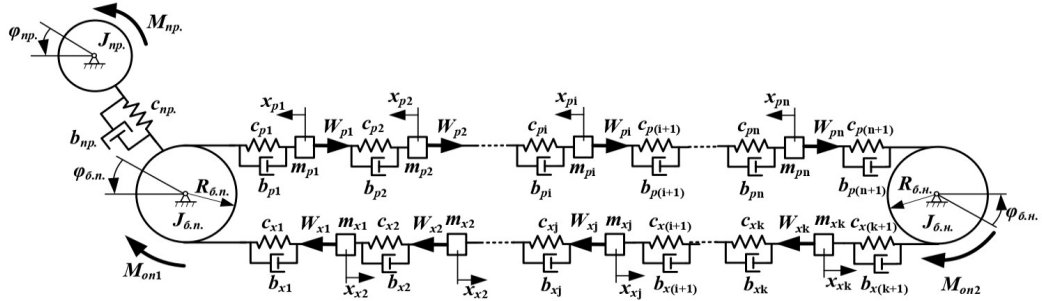


Fig. 1. Belt conveyor dynamical model

In the current investigation, we accept it without any changes. In Fig. 1 the following designations are made: M_{np} – reduced torque of the drive (all the values are reduced to the drive drum); M_{on1} and M_{on2} – reduced torques of the resistance forces, which act on the drive drum and take-up drum respectively; c_{np} – reduced coefficient of the torsional stiffness of the drive; b_{np} – reduced coefficient of the torsional dissipation of the drive; $R_{\delta.n.}$ and $R_{\delta.h.}$ – radii of the drive and take-up drums respectively; J_n , $J_{\delta.n.}$, $J_{\delta.h.}$ – reduced moments of inertia of the drive, drive drum, and take-up drum respectively; m_{pi} – i -th reduced mass of the upper (loaded) strand; m_{xj} – j -th reduced mass of the lower (unloaded) strand; n and k – total number of the reduced masses of the upper and lower strands respectively; c_{pi} and b_{pi} – i -th reduced coefficients of stiffness and dissipation of the upper strand (between neighboring reduced masses); c_{xj} and b_{xj} – j -th reduced coefficients of stiffness and dissipation of the lower strand; W_{pi} and W_{xj} – i -th and j -th reduced friction forces, which are caused by the idlers' rotation. Taking into consideration the dynamical model (Fig. 1) corresponding mathematical model may be presented as follows [10]:

A dot under character denotes a derivative by time. Note, that similar belt conveyor models are presented in the works [4, 10].

Since mathematical model (1) is quite complicated we should explain it more carefully. The parallel connection of c_{np} and b_{np} (Fig. 1) reflects the belt transmission of the conveyor drive. All the inertial elements (coupling, shaft of a motor) from its left side are reduced to J_{np} . All the elements from its right side (coupling and drive drum) are reduced to $J_{\delta.n.}$. Thus, all the dynamical features of the drive are taken into account

The belt itself is presented as a chain structure of reduced masses $m_{p,i}$ (upper strand) or $m_{x,j}$ (lower strand). The bulk material rides on the upper strand. That is why we set $n=20$ and $k=4$. Reduced masses $m_{p,i}$ and $m_{x,j}$ are connected with the elements with stiffness and dissipation features. Thereby, damped oscillations of the belt may be studied with the model (1). Resistance force $W_{p,i}$ or $W_{x,j}$ act on each element $m_{p,i}$ or $m_{x,j}$. Torques M_{on1} and M_{on2} , which are caused by

friction, are taken into account as well. They influence the overall power consumption.

$$\left\{
 \begin{aligned}
 M_{np} &= \ddot{\varphi}_{np} J_{np} + c_{np} (\varphi_{np} - \varphi_{\delta,n}) + b_{np} (\dot{\varphi}_{np} - \dot{\varphi}_{\delta,n}); \\
 c_{np} (\varphi_{np} - \varphi_{\delta,n}) + b_{np} (\dot{\varphi}_{np} - \dot{\varphi}_{\delta,n}) &= \ddot{\varphi}_{\delta,n} J_{\delta,n} + M_{on,1} + c_{p1} (\varphi_{\delta,n} R_{\delta,n} - x_{p1}) + \\
 &+ b_{p1} (\dot{\varphi}_{\delta,n} R_{\delta,n} - \dot{x}_{p1}) + c_{x1} (\varphi_{\delta,n} R_{\delta,n} - x_{x1}) + b_{x1} (\dot{\varphi}_{\delta,n} R_{\delta,n} - \dot{x}_{x1}); \\
 c_{p1} (\varphi_{\delta,n} R_{\delta,n} - x_{p1}) + b_{p1} (\dot{\varphi}_{\delta,n} R_{\delta,n} - \dot{x}_{p1}) &= m_{p1} \ddot{x}_{p1} + W_{p1} + c_{p2} (x_{p1} - x_{p2}) + \\
 &+ b_{p1} (\dot{x}_{p1} - \dot{x}_{p2}); \\
 \dots \\
 c_{pi} (x_{p(i-1)} - x_{pi}) + b_{pi} (\dot{x}_{p(i-1)} - \dot{x}_{pi}) &= m_{p1} \ddot{x}_{p1} + W_{p1} + c_{p(i+1)} (x_{pi} - x_{p(i+1)}) + \\
 &+ b_{p(i+1)} (\dot{x}_{pi} - \dot{x}_{p(i+1)}), \quad i = \overline{(2, n-1)}; \\
 \dots \\
 c_{pn} (x_{p(n-1)} - x_{pn}) + b(\dot{x}_{p(n-1)} - \dot{x}_{pn}) &= m_{pn} \ddot{x}_{pn} + W_{pn} + c_{p(n+1)} (x_{pn} - \varphi_{\delta,n} R_{\delta,n}) + \quad (1) \\
 &+ b_{p(n+1)} (\dot{x}_{pn} - \dot{\varphi}_{\delta,n} R_{\delta,n}); \\
 R_{\delta,n} (c_{p(n+1)} (x_{pn} - \varphi_{\delta,n} R_{\delta,n}) + b_{p(n+1)} (\dot{x}_{pn} - \dot{\varphi}_{\delta,n} R_{\delta,n})) &= c_{x(k+1)} (\varphi_{\delta,n} R_{\delta,n} - x_{x(k+1)}) + \\
 &+ b_{x(k+1)} (\dot{\varphi}_{\delta,n} R_{\delta,n} - \dot{x}_{x(k+1)}) + \ddot{\varphi}_{\delta,n} J_{\delta,n} + M_{on,2}; \\
 c_{x(k+1)} (\varphi_{\delta,n} R_{\delta,n} - x_{x(k+1)}) + b_{x(k+1)} (\dot{\varphi}_{\delta,n} R_{\delta,n} - \dot{x}_{x(k+1)}) &= W_{xk} + m_{xk} \ddot{x}_{xk} + c_{xk} (x_{xk} - x_{x(k-1)}) + \\
 &+ b_{xk} (\dot{x}_{xk} - \dot{x}_{x(k-1)}); \\
 \dots \\
 c_{x(j+1)} (x_{x(j+1)} - x_{xj}) + b_{x(j+1)} (\dot{x}_{x(j+1)} - \dot{x}_{xj}) &= m_{xj} \ddot{x}_{xj} + W_{xj} + c_{xj} (x_{xj} - x_{x(j-1)}) + \\
 &+ b_{xj} (\dot{x}_{xj} - \dot{x}_{x(j-1)}), \quad j = \overline{(2, k-1)}; \\
 \dots \\
 c_{x2} (x_{x2} - x_{x1}) + b_{x2} (\dot{x}_{x2} - \dot{x}_{x1}) &= m_{x1} \ddot{x}_{x1} + W_{x1} + c_{x1} (x_{x1} - R_{\delta,n} \varphi_{\delta,n}) + b_{x1} (\dot{x}_{x1} - R_{\delta,n} \dot{\varphi}_{\delta,n}).
 \end{aligned}
 \right.$$

Mathematical model (1) was obtained via the application of the d'Alembert-Lagrange principle. Each of the equations in the system (1) is presented in such a manner, that from the left side of an equal sign driven factors are placed, from the right side all the resistance factors are collected.

We consider a start process. Thus, at the moment $t=0$ all the mechanical elements of the conveyer are in the rest:

$$\left\{
 \begin{aligned}
 \varphi_{np}(0) &= \varphi_{\delta,n}(0) = x_{pi}(0) = x_{xj}(0) = \varphi_{\delta,n}(0) = 0; \\
 \dot{\varphi}_{np}(0) &= \dot{\varphi}_{\delta,n}(0) = \dot{x}_{pi}(0) = \dot{x}_{xj}(0) = \dot{\varphi}_{\delta,n}(0) = 0.
 \end{aligned} \quad (2)
 \right.$$

One of the main factors, which determines the dynamical and energy features of the belt conveyor start, is the driving torque, caused by the conveyor's asynchronous motor. In the current study we use a stationary (referred to the stator) system of coordinates [11], the corresponding system of equations follows:

$$\begin{cases} \frac{di_{1\alpha}}{dt} = \frac{1}{\delta L_1} (u_{1\alpha} - i_{1\alpha} R_1 + k_2 e_{2\alpha}); \\ \frac{di_{1\beta}}{dt} = \frac{1}{\delta L_1} (u_{1\beta} - i_{1\beta} R_1 - k_2 e_{2\beta}); \\ \frac{di_{2\alpha}}{dt} = -\frac{1}{\delta L_2} ((u_{1\alpha} - i_{1\alpha} R_1) k_1 + e_{2\alpha}); \\ \frac{di_{2\beta}}{dt} = -\frac{1}{\delta L_2} ((u_{1\beta} - i_{1\beta} R_1) k_1 - e_{2\beta}); \\ M_{np.} = U \eta \frac{3}{2} p L_{12} (i_{1\beta} i_{2\alpha} - i_{1\alpha} i_{2\beta}), \end{cases} \quad (3)$$

where $i_{1\alpha}$, $i_{1\beta}$ – projections of the stator current generalized vector on the stationary orthogonal axes α and β respectively; $i_{2\alpha}$, $i_{2\beta}$ – projections of the rotor current generalized vector on the axes α and β respectively; L_1 , L_2 – induction coefficients of the stator and rotor windings respectively; L_{12} – coefficient of mutual induction; k_1 and k_2 – coefficients of the magnetic coupling of stator and rotor respectively ($k_1=L_{12}L_1^{-1}$; $k_2=L_{12}L_2^{-1}$); p – number of poles' pairs of the motor; $u_{1\alpha}$, $u_{1\beta}$ – projections of stator voltage generalized vector on the axes α and β ($u_{1\alpha}=U_{\max}\cos(2\pi f dt)$, $u_{1\beta}=U_{\max}\sin(2\pi f dt)$); U_{\max} – magnitude of the line-to-ground voltage of the motor; f – frequency of the voltage ($f=\text{const}$); $e_{2\beta}$, $e_{2\alpha}$ – EMFs, which are inducted by the rotor flux linkage on the axes α and β respectively ($e_{2\alpha}=p\omega_{\text{oe}}(L_2 i_{2\beta} + L_{12} i_{1\beta}) + i_{2\alpha} R_2$, $e_{2\beta}=p\omega_{\text{oe}}(L_2 i_{2\alpha} + L_{12} i_{1\alpha}) + i_{2\beta} R_2$); R_1 – active impedance of the stator winding; R_2 – active impedance of the rotor winding; X_1 – inductive impedance of the stator winding; X_2 – inductive impedance of the rotor winding; δ – magnetic leakage coefficient ($\delta=1-(1+X_1(2\pi f L_{12})^{-1}(1+X_2(2\pi f L_{12})^{-1})^{-1}$); ω_{oe} – angular velocity of the motor; U – overall reduction ratio of the conveyor transmission; η – efficiency of the conveyor transmission. All electrical values are reduced to the stator winding.

We accept that all the electrical processes in the motor at the moment $t=0$ are absent. Thus, the initial condition for currents are as follows:

$$i_{1\alpha}(0) = i_{1\beta}(0) = i_{2\alpha}(0) = i_{2\beta}(0) = 0. \quad (4)$$

A soft-starter provides a power supply to the conveyor motor. Thus, during a start the magnitude of the motor voltage follows the ramped law:

$$U_{\max} = U_{0,\max} + (U_{\text{nom. max}} - U_{0,\max}) \frac{t}{t_p}, \quad (5)$$

where $U_{0,\max}$ – initial amplitude of the voltage; t – time; t_p – duration of the voltage increasing from $U_{0,\max}$ to $U_{\text{nom},\max}$; $U_{\text{nom},\max}$ – magnitude of the voltage under line supply. The tunable parameters of a soft-starter are t_p and $U_{0,\max}$.

Soft-starters are commonly used as power supply units for asynchronous drives. Their using limits electromagnetic torque (it, in turn, increases the lifetime of mechanical elements of machines: couplings, shafts, etc.) and current in the stator winding. Since the belt is the element with the lowest reliability, we require a limitation of the maximum force in the belt. The second constraint is connected with the current limitation:

$$\begin{cases} \frac{F_{b,\max}}{F_{b,st}} = \frac{\max(c_{p1}(\varphi_{\delta,n}(t)R_{\delta,n} - x_{p1}(t)) + b_{p1}(\dot{\varphi}_{\delta,n}(t)R_{\delta,n} - \dot{x}_{p1}(t)))}{c_{p1}(\varphi_{\delta,n}(t_p)R_{\delta,n} - x_{p1}(t_p)) + b_{p1}(\dot{\varphi}_{\delta,n}(t_p)R_{\delta,n} - \dot{x}_{p1}(t_p))} \leq \lambda_1, \\ \frac{i_{1\alpha,\max}}{i_{1\alpha,st}} = \frac{\max(\sqrt{i_{1\alpha}^2(t) + i_{1\beta}^2(t)})}{\sqrt{i_{1\alpha}^2(t_p) + i_{1\beta}^2(t_p)}} \leq \lambda_2, \end{cases} \quad (6)$$

where $F_{b,\max}$ and $F_{b,st}$ – maximal and static forces of the belt during conveyor start (the force in the upper belt where it climbs onto the drive drum); $i_{\alpha,\max}$ and $i_{\alpha,st}$ – maximal and static values of projection of the stator current generalized vector on the axis α ; λ_1 and λ_2 – values, that determine acceptable ratios of the belt forces and stator currents respectively (in the current work we set $\lambda_1=1.005$, $\lambda_2=2.350$).

The static values in (6) correspond to the end of the start. Indeed, since a commonly tuned start duration is longer, than 5 seconds, all the mechanical and electrical transient processes are finished. Other important constraints (maximal electromagnetic torque, maximal torque in transmission, maximal power, maximal losses of energy, etc.) may be involved in the calculations [12]. RMS's values are reasonable alternative to maximal indicators.

The optimization problem requires the following criterion to be minimized:

$$\Delta E = \frac{3}{2} \int_0^{t_p} (R_1(i_{1\beta}^2 + i_{1\alpha}^2) + R_2(i_{2\beta}^2 + i_{2\alpha}^2)) dt \rightarrow \min, \quad (7)$$

where ΔE – overall energy losses in the drive, that are caused by heating of the stator and rotor windings. The importance of the ΔE minimization is caused by the need of drive energy efficiency increasing.

The sense of the optimization problem is as follows: numerical values of $U_{0,\max}$ and t_p must be determined, in a way that constraints (6) are satisfied and criterion (7) is minimized. The statement of the problem may be extended by the inclusion of additional constraints (we have pointed out some examples) and additional criteria. In that case, we will obtain a complex optimization problem. However, the methodology, developed in further, remains the same.

Constraints (6) and criterion (7) are implicitly dependent on the non-linear mathematical model of the system (1), (3). In order to calculate numerical values

$\frac{F_{b.\max}}{F_{b.st}}$, $\frac{i_{1\alpha.\max}}{i_{1\alpha.st}}$ and ΔE we should set values $U_{0.\max}$ and t_p and numerically integrate differential equations (1), (3). Thus, the first step of the problem solution is the development of a function $f_{\text{model} \rightarrow \text{solution}}$. Found functions $i_{1\alpha}$, $i_{1\beta}$, $i_{2\alpha}$, $i_{2\beta}$, x_{xj} , x_{pi} , φ_{np} , $\varphi_{\delta.n}$, $\varphi_{\delta.H}$ allow to calculate criterion (7) value and fractions $\frac{F_{b.\max}}{F_{b.st}}$, $\frac{i_{1\alpha.\max}}{i_{1\alpha.st}}$.

Since they have different units we should reduce them to non-dimension forms. Thus, we use $\frac{\Delta E}{E_k}$ value (where E_k – is the total kinetic energy of the system) to present criterion (7) quantity. The next step is the development of a function $f_{\text{solution} \rightarrow \text{criterion, constraints}}$, that is fed by functions $i_{1\alpha}$, $i_{1\beta}$, $i_{2\alpha}$, $i_{2\beta}$, x_{xj} , x_{pi} , φ_{np} , $\varphi_{\delta.n}$, $\varphi_{\delta.H}$. Its outputs are $\frac{\Delta E}{E_k}$, $\frac{F_{b.\max}}{F_{b.st}}$ and $\frac{i_{1\alpha.\max}}{i_{1\alpha.st}}$. In order to carry out the optimization procedure, obtained values $\frac{\Delta E}{E_k}$, $\frac{F_{b.\max}}{F_{b.st}}$ and $\frac{i_{1\alpha.\max}}{i_{1\alpha.st}}$ should be reduced to one form. Such reduction may be executed with the following generalized criterion:

$$Cr = \frac{\Delta E}{E_k} + In_1 + In_2 \rightarrow \min, \quad (8)$$

where In_1 and In_2 – are terms, which take into account inequalities (6):

$$In_1 = \delta_F \begin{cases} 0, & \frac{F_{b.\max}}{F_{b.st}} \leq \lambda_1; \\ \frac{F_{b.\max}}{F_{b.st}}, & \frac{F_{b.\max}}{F_{b.st}} > \lambda_1; \end{cases} \quad (9)$$

$$In_2 = \delta_i \begin{cases} 0, & \frac{i_{1\alpha.\max}}{i_{1\alpha.st}} \leq \lambda_2; \\ \frac{i_{1\alpha.\max}}{i_{1\alpha.st}}, & \frac{i_{1\alpha.\max}}{i_{1\alpha.st}} > \lambda_2, \end{cases} \quad (10)$$

where δ_F and δ_i – weight coefficients, which form the criterion (8) desired topology.

The following recommendation must be met $\delta_F \gg \delta_i \gg 1$. In the frame of the current study $\delta_F = 10^8$, and $\delta_i = 10^6$. Such values form a „pit in pit” criterion (8) topology. The upper pit has a topology of the fraction $\frac{F_{b.\max}}{F_{b.st}}$. If the optimization algorithm finds the solution, which satisfies the first constraint (6), then the term In_1 becomes zero. Further search is continued in the middle pit. It has the topology

of the fraction $\frac{i_{1\alpha,\max}}{i_{1\alpha,st}}$. Satisfaction of the second constraint (6) makes the term In_2 equal to zero and only component $\frac{\Delta E}{E_k}$ remains. Such sequential search is provided by the weight coefficients δ_F, δ_i values.

All of the described calculations should be carried out in the function $f_{\text{criterion, constraints} \rightarrow \text{generalized criterion}}$. Cascade of the functions $f_{\text{model} \rightarrow \text{solution}}$, $f_{\text{solution} \rightarrow \text{criterion, constraints}}$, $f_{\text{criterion, constraints} \rightarrow \text{generalized criterion}}$ may be presented in the compact form (Fig. 2) as an objective function $f_{\text{OF}}(U_{0,\max}, t_p)$ to minimize.

Thus, we reduced the initial optimization problem with constraints (6) to the unconstrained one (8). It provides the basis for an optimization algorithm application.

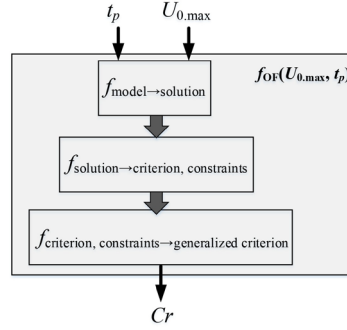


Fig. 2. Schematic illustration of the objective function f_{OF}

3. Results

Since the objective function is built, we may run the optimization procedure. We should ground optimization method, that will be applied. One of the methods, that was developed and studied in the work [13] is a modification of PSO with a rotating ring topology of connections between particles (PSO-Rot-Ring). The algorithm PSO-Rot-Ring showed promising results for a bunch of complicated benchmark functions [13]. The objective function f_{OF} of the current research has a difficult topology as well. To show all function f_{OF} pits 3-d plots are shown (Fig. 3). Function f_{OF} minimum is located at the edge of the lower pit, right where the wall of the constraint (10) and the sloping surface of the component $\frac{\Delta E}{E_k}$ form a canyon (Fig. 3, b). Searching of the minimum point in the narrow canyon is a difficult problem.

All the calculations were executed for a belt conveyor with a capacity 100 ton/h, a length of conveying equals 45 m. All the numerical values of parameters follow $c_{np}=2850$ Nm/rad, $b_{np}=5000$ Nms/rad, $R_{\delta,n}=R_{\delta,h}=0.2$ m, $J_n=15.29$ kgm², $J_{\delta,n}=J_{\delta,h}=2.8$ kgm², $m_{pi}=21.25$ kg, $m_{xj}=6.25$ kg, $c_{pi}=180$ kN/m, $b_{pi}=b_{xj}=500$ Ns/m, $c_{xj}=36$ kN/m, $W_{pi}=19$ N, $W_{xj}=4.5$ N, $L_1=0.0082$ H, $L_2=0.0014$ H, $L_{12}=0.295$ H,

$k_1=0.97$, $k_2=0.99$, $p=2$, $f=50$ Hz, $R_1=2.12$ Ω , $R_2=1.36$ Ω , $X_1=2.58$ Ω , $X_2=0.43$ Ω , $\delta=0.0316$, $U=18$, $\eta=0.9$.

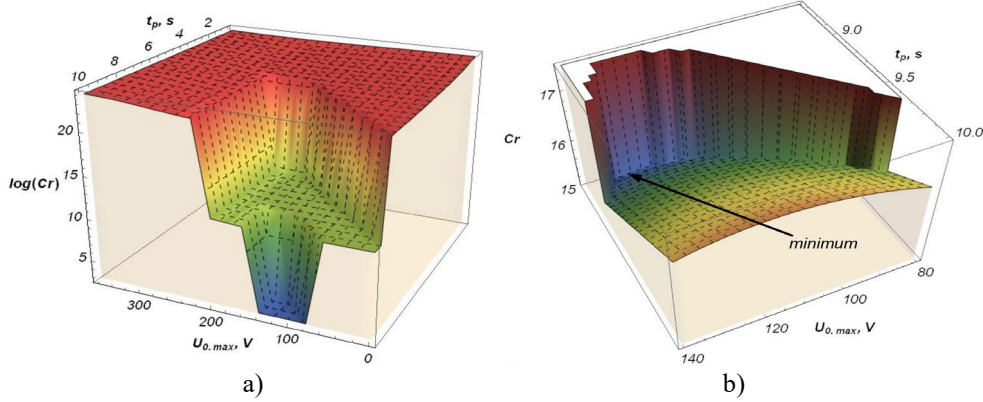


Fig. 3. Topology of the function f_{OF} : a) overall domain ($t_p \in [1, 10]$, $U_0 \in [20, 360]$); b) area of

the lowest pit, which reflects only $\frac{\Delta E}{E_k}$ component

The swarm population (SP) equals 10 and we set 40 iterations ($Iter$) for the PSO-Rot-Ring algorithm. Algorithm application brought following values: $U_{0,max}=129.93$ V, $t_p=8.68$ s.

Since PSO-Rot-Ring algorithm provides stochastic optimization, found values $U_{0,max}$ and t_p may not refer to the function f_{OF} minimum. In order to be sure about those, PSO-Rot-Ring sensitivity analysis was carried out. PSO-Rot-Ring algorithm was run 30 times (a round), each time with different initialization of arguments $U_{0,max}$ and t_p . Median value of the function f_{OF} was chosen as a round output. For each round values SP and $Iter$ were different. Calculated numbers of $U_{0,max}$ and t_p (outputs) are given in Table 1.

Table 1

Calculated values $U_{0,max}$ and t_p as a result of PSO-Rot-Ring application

Iter	SP				
	5	10	15	20	40
20	115.02 V 1.81 s	120.98 V 4.44 s	128.96 V 8.92 s	129.03 V 8.92 s	129.13 V 8.95 s
40	124.44 V 8.65 s			129.93 V	
60	129.92 V 8.68 s			8.68 s	

One may observe from Table 1 poor algorithm performance when small SP and $Iter$. PSO-Rot-Ring could not find f_{OF} minimum. Convergence plots (Fig. 4) support this statement. Indeed, for the case $SP=5$ algorithm could not find even criterion (8) middle pit. For the case $SP=10$ a swarm slid down to the lower pit at the sixth iteration. For the case $SP=40$ algorithm found a lower pit at the very first iteration. The rest of iterations were spent for accurate determination of minimum

location. After the tenth iteration, there was no improvement of criterion (8) value, i.e. further iterations are useless.

All these data support the statement about the minor influence of values SP and $Iter$ on PSO-Rot-Ring performance for the case $10 \leq SP, 40 \leq Iter$. Thus, to avoid useless calculations, we may recommend setting $SP=10$, $Iter=40$ for similar problems.

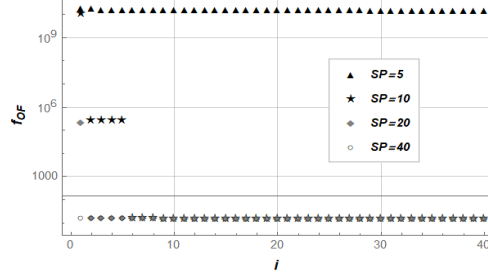


Fig. 4. Convergence curves of PSO-Rot-Ring algorithm

4. Discussion

In order to show the achieved effect, caused by soft-starter optimal settings, we presented numerical values of the energy and dynamic indicators of the conveyor start (Table 2).

Table 2

Numerical values of conveyor start indicators

Options		Indicators		
$U_{0,max}$, V	t_p , s	$\frac{F_{b,max}}{F_{b,st}}$	$\frac{i_{1\alpha,max}}{i_{1\alpha,st}}$	$\frac{\Delta E}{E_k}$
100	1	1.939	3.787	4.521
	2	1.420	2.939	5.915
	5	1.032	2.531	9.951
	10	1.002	2.327	16.925
200	1	1.640	3.543	4.683
	2	1.386	3.199	5.892
	5	1.019	3.011	9.238
	10	1.001	2.999	14.745
300	1	2.223	4.261	4.281
	2	2.085	4.511	5.079
	5	2.005	4.510	7.246
	10	1.979	4.506	10.779
Optimal values		1.002	2.326	15.313

Presented in Table 2 values clearly show the influence of parameters $U_{0,max}$ and t_p on energy and dynamic indicators. Analysis of the data leads to the following conclusions: the bigger duration t_p , the smaller value $\frac{F_{b,max}}{F_{b,st}}$; the bigger

value of $U_{0,\max}$, the smaller $\frac{i_{1\alpha,\max}}{i_{1\alpha,st}}$ (the only exception, which is recorded in Table 2, refers to the case $U_{0,\max}=300$ V); increase of $U_{0,\max}$ (up to the value 300 V) and t_p cause the increase of the value $\frac{\Delta E}{E_k}$.

All of the mentioned above relationships are nonlinear. Thus, as it was mentioned in the introduction, the determination of optimal tuning soft-starter parameters is not a simple problem.

In order to show the most important characteristics, which refer to the optimally tuned soft-starter, the plots were built (Fig. 5).

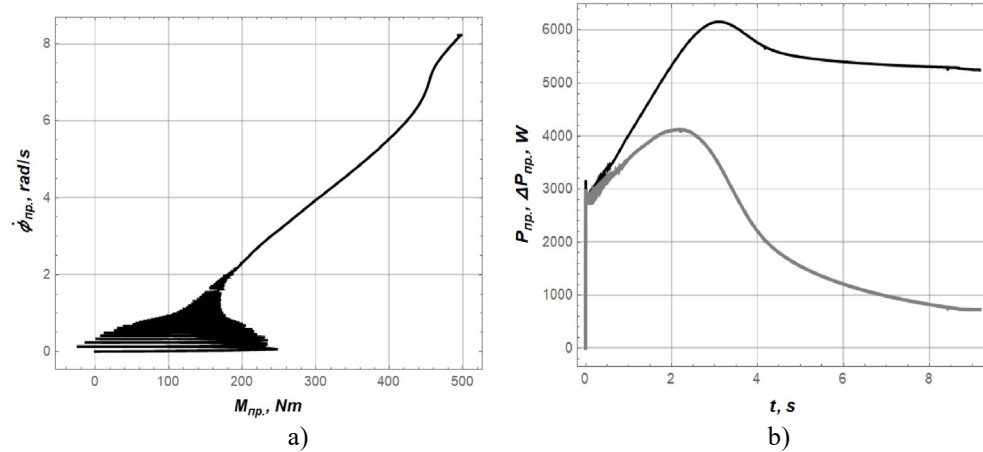


Fig. 5. Characteristics of belt conveyor start under the optimally tuned soft-starter control:
a) speed/torque characteristic of the asynchronous motor; b) consumed power of the drive (black curve) and power losses in the drive (gray curve)

The supplied voltage U_{\max} influences the change of torque-angular velocity characteristic (Fig. 5, a). After the initial oscillation part, it increases up to the steady torque at the end of the start. Analysis of the energy features (Fig. 5, b) shows a heavy start. Indeed, curves P_{np} and ΔP_{np} are almost merged during the first seconds of the start. It is quite ineffective. For instance, at the moment $t=2.1$ s efficiency coefficient equals 26.4%. However, taking in mind constraints (9), (10), and limited soft-starter technical capabilities, we may state: this is the best result. Changing constraints or/and criterion to minimize brings another set of belt conveyor start features.

5. Conclusions

1. Stated in the article problem includes the mathematical model of the system and initial conditions; two constraints, which limit the magnitude of the current and the maximal force in the belt; criterion to minimize (energy losses). The voltage of the drive is a control. Its varying is characterized by the initial value $U_{0,\max}$ and duration of increasing t_p , which must be determined.

2. In order to reduce the initial problem to the unconstrained one, we applied the approach, which consists in the objective function development with a „pit in pit” topology. Such a nesting led to constraints satisfaction and energy losses criterion minimization.
3. PSO-Rot-Ring algorithm was applied to find the objective function minimum. The found values are $U_{0,\max} = 129.93$ V, $t_p = 8.68$ s. They may be inserted into a soft-starter manual as recommendations to follow.
4. Developed in the article approach may be generalized by considering a wide domain of laws of voltage increasing, including voltage impacts at the beginning of the start (their duration and magnitude should be found), etc. The deeper level of investigation should involve algorithms of soft-starter operation (in particular, switching of the bidirectional thyristors). In addition, the developed in the article methodology might be applied to other machinery, i.e. screw, bucket, chain-and-flight conveyors, etc.

R E F E R E N C E S

- [1]. *Y. Shengzhe, Y. Yan, Y. Ning*. “Analysis and Comparison of Soft-start Systems Applied to Belt Conveyors” in Applied Mechanics and Materials, **vol. 321-324**, 2013, pp. 1597-1601
- [2]. *X. Guo, B Liu* “Research on Energy-Saving Optimization Control System of Mine Belt Conveyor” in 2019 International Conference on Robots & Intelligent System (ICRIS), Haikou, China, 15-16 June 2019, INSPEC Accession Number: **18940313**, 2019, pp. 46-49.
- [3]. *F. Zeng, C. Yan, Q. Wu et. al.* “Dynamic Behaviour of a Conveyor Belt Considering Non-Uniform Bulk Material Distribution for Speed Control” in Applied Sciences, **vol. 10(13)**, 2020, p. 4436.
- [4]. *F. Yu, Z. Miaotian, L. Guoping, M. Guoying* “Dynamic characteristic analysis and startup optimization design of an intermediate drive belt conveyor with non-uniform load” in Science Progress, **vol. 103(1)**, 2019, pp. 1-20.
- [5]. *O. Pihnastyi, V. Khodusov* “Development of the controlling speed algorithm of the conveyor belt based on TOU tariffs” in CEUR Workshop Proceedings. Information-Communication Technologies & Embedded Systems (ICTES 2020), Mykolaiv, Ukraine, **vol. 2762**, 2020, pp. 73-86.
- [6]. *V. Dmitrieva, P. Sizin, A. Sobyanin* “Application of the soft starter for the asynchronous motor of the belt conveyor” in IOP Conf. Series: Earth and Environmental Science, Wroclaw, Poland, 23-25 June 2021, **paper no. 942 012003**, 2021, pp. 1-11.
- [7]. *L. Yunxia, L. Lei, C. Zhang* “AMT Starting Control as a Soft Starter for Belt Conveyors Using a Data-Driven Method” in Symmetry, **vol. 13**, 2021, pp. 1-18.
- [8]. *L. Yunxia, L. Lei* “Research on segmented belt acceleration curve based on automated mechanical transmission” in Processes, **vol. 10(106)**, 2022, pp. 1-18.
- [9]. *P. Nayak, T. Rufzal* “Performance analysis of feedback controller design for induction motor soft-starting using bio-inspired algorithms” in 2018 International Conference on Power, Instrumentation, Control and Computing (PICC), Thrissur, India, 18-20 January 2018, INSPEC Accession Number: **17843400**, 2018, pp. 1-6.
- [10]. *V. Loveykin, Y. Romasevych* “Mathematical modeling of belt conveyor movement” in Lifting and Conveying Machinery, **vol. 2**, 2017, pp. 16-23 (in Ukrainian)
- [11]. *H. Razik* “Handbook of asynchronous machines with variable speed”. 1st ed – London: John Wiley & Sons, Inc., 2011. – p. 409.
- [12]. *A. Menaem, M. Elgamal, A.-H. Abdel-Aty et al.* “A proposed ANN-based acceleration control scheme for soft starting induction motor” in IEEE Access, **vol. 9**. INSPEC Accession Number: **20322987**, 2020, pp. 4253-4265.
- [13]. *Y. Romasevych, V. Loveykin Y.* “Loveykin Development of New Rotating Ring Topology of PSO-Algorithm” in 2021 IEEE 2nd KhPI Week on Advanced Technology (KhPIWeek), Kharkiv, Ukraine, 13-17 September 2021, INSPEC Accession Number: **21460319**, pp. 79-82.